The Egyptian Journal of Radiology and Nuclear Medicine 47 (2016) 1539–1548

Contents lists available at ScienceDirect

The Egyptian Journal of Radiology and Nuclear Medicine

journal homepage: www.sciencedirect.com/locate/ejrnm

Original Article

Preoperative glioma grading by MR diffusion and MR spectroscopic imaging

Faten Mohamed Fawzy [a], Hosam N. Almassry [a,*], Ayman M. Ismail [b]

[a] Radiodiagnosis Department, Zagazig University Hospitals, Egypt
[b] Neurosurgery Department, Zagazig University Hospitals, Egypt

ARTICLE INFO

Article history:
Received 5 June 2016
Accepted 10 July 2016
Available online 25 August 2016

Keywords:
Glioma grading
DWI
ADC
MRS
GBM

ABSTRACT

Objectives: To assess the diagnostic accuracy of DW-MRI, ADC value, and MRS in preoperative glioma grading because of its importance in treatment planning.
Patients and methods: A prospective study included 30 patients with gliomas, based on CT and cMRI findings, referred from Neurosurgery Department for DWI and MRS. Results were correlated with histopathological diagnosis after surgical resection.
Results: ADC values were significantly higher in low grade gliomas relative to high grade ones. The lowest value was for GBM, 100% sensitivity, specificity, PPV and NPP in glioma grading. MRS revealed higher Cho/NAA and Cho/Cr ratios in high grade neoplasms and characteristic elevated lipid peak with statistical significant difference between low grade and high grade gliomas. MRS was more accurate than ADC value in detecting peritumoral infiltration of high grade gliomas, but there were no statistically significant differences between anaplastic and GBM in tumoral and peritumoral regions.
Conclusion: DW-MRI had higher sensitivity, specificity and accuracy than cMRI and MRS in glioma grading while MRS is more accurate than ADC value in assessing peri-tumoral infiltration based on high metabolite ratios in peri-tumoral tissue for anaplastic glioma and GBM, but there were no statistically significant differences between high grade groups.

1. Introduction

Accurate glioma grading is a cornerstone for management strategic planning and treatment options; over estimation of glioma grading may be harmful for some patients who can be subjected to unnecessary adjuvant therapy, whereas under estimation of glioma grading can lead others to lose their chances for proper management with concomitant morbidity and mortality [1,2].

Although histopathological grading is the current reference standard, yet the results may be inaccurate when biopsy samples are not taken from the most malignant part of the tumor or when the tumor is not completely resected [3].

The most important predictors of tumor grading are mass effect and the presence of necrosis. Contrast enhancement is also considered as a predictor for high grade gliomas as it signifies blood-brain barrier breakdown; however, it may be deceiving in grading decision as high grade glioma may be misdiagnosed as a low grade one when it demonstrates minimal edema, without contrast enhancement, necrosis, or mass effect. Conversely,

Peer review under responsibility of The Egyptian Society of Radiology and Nuclear Medicine.
* Corresponding author.
E-mail addresses: fatenfawzy25@hotmail.com (F.M. Fawzy), hosamelmassry@gmail.com (H.N. Almassry), aymanmismael@gmail.com (A.M. Ismail).

http://dx.doi.org/10.1016/j.ejrnm.2016.07.006
0378-603X/

low grade glioma may sometimes demonstrates criteria of high grade glioma as peri-tumoral edema, contrast enhancement, and mass effect [4].

Non-invasive grading of tumor cellularity can be achieved by DW-MR imaging; as the tumor cells comprise a relative barrier to water diffusion, so water diffusibility is low in high cellular tumors than in low cellular ones [5,6]. Expectedly the ADC value is low in more cellular tumors than in tumors of low cellular components [6]. The lower ADC values are now accepted as a marker of higher grade gliomas, and higher ADC values suggest low grade gliomas [7].

Proton MR Spectroscopy is a noninvasive tool for detecting metabolic alteration in brain lesions and to detect specific patterns in the changes of metabolite concentrations compared with those in normal brain [8]. It allows reliable differentiation of tumor margin from adjacent brain parenchymal edema which is not possible with gadolinium-enhanced MRI that underestimates or overestimates tumor size in approximately 40% of cases [9,10]. Unfortunately, there are no equivocal cutoff metabolite signal ratios that clearly distinguish neoplastic from non-neoplastic conditions [2].

Analysis of Lipid metabolite peak can also aid in grading primary neoplasms as high grade neoplasms tend to have elevated lipid signal, which is often absent in low grade neoplasms [11]. On the other hand, a high myoinositol peak is more characteristic for lower grade neoplasms and gliomatosis cerebri [12].

Lipid resonance has been observed in high grade gliomas in vivo, using different echo times, especially in areas of MRI-detectable necrosis. Necrosis distinguishes high from low grade gliomas in the majority of the histologic classification systems and correlate inversely with survival time [13,14].

The aim of this study was to evaluate the diagnostic accuracy of DW-MRI and MRS in glioma grading.

2. Patient and methods

This prospective study was carried out during the period from January 2015 to February 2016 and included thirty patients proved to have intra-axial SOL of glial origin based on CT and conventional MR findings and referred to Radiodiagnosis Department from Neurosurgery Department of Zagazig University Hospitals. They were 18 males and 12 females, and their ages ranged from 6 to 76 years.

The study was approved by our institutional ethics committees and a written consent was obtained from each patient, and from the first degree relatives of the pediatric patients, before participating in the study.

2.1. I-MR Imaging Protocol;

2.1.1. Conventional magnetic resonance imaging (cMRI)

All MRI studies were done using Philips MR machine (1.5 Tesla). The contrast media used were either Omniscan or Magnevist [Gadolinium (Diethylene Triamine Penta Acidic acid) (“Gd-DTPA”)], and it was administrated intravenously in a dose of 0.1 mmol/kg body weight (0.2 ml/kg). T1-WIs were obtained immediately after the end of contrast injection in axial, coronal and sagittal planes. According to the conventional MR imaging findings, glioma grading was based on their appearance on different MR sequences using the following criteria: border definition, signal intensity (homogeneity/heterogeneity), hemorrhage, necrosis or breakdown, grade of perilesional edema, contrast enhancement pattern and mass effect.

2.1.2. Advanced magnetic resonance imaging

(a) Diffusion Weighted MR Imaging (DW-MRI):

The imaging sequence for DW-MRI was a multi-sectional single shot spin echo EPI sequence (TR/TE/NEX: 4200/140 ms/1) with diffusion sensitivities of b values = 0, 1000 s/mm^2.

The ADC maps were calculated automatically by MRI software and included in the sequence. Measurements of ADC were made in different regions of interest (ROI) of the lesions and in comparable contralateral regions. The ADC values were expressed in 10^{-3} mm^2/sec.

(b) Proton MR Spectroscopy:

Selection of the MR spectroscopy technique (single voxel spectroscopy (SVS) versus chemical shift imaging (CSI)), depended primarily on the appearance of the lesion in the preceding pre and post-contrast MR images. Water suppression of the dominant water signal was done by CHESS technique (Chemical shift selective pulse).

Frequency domain curve was fitted by the manufacturer to define N-acetyl aspartate (NAA), Choline-containing components (Cho), and Creatine and Phosphocreatine (Cr) peaks.

Patient spectra were interpreted qualitatively by inspection of the peaks and determination of any peak changes compared to other control spectra of the same patient. Another approach is the quantitative approach using the integral metabolite ratios.

(i) Single Voxel Spectroscopy (SVS)

The voxel was placed in the indeterminate area identified on the axial post contrast T1WIs and in a comparable contralateral region. Voxel size was chosen to provide adequate signal and to be small enough to prevent partial volume averaging of adjacent structures. Voxel sizes varied between 1.5 and 2 ccm.

Point resolved spectroscopy (PRESS) pulse sequence was used for volume localization, because of its improved S/N ratio, and less sensitivity to motion and to multiple quantum effects.

(ii) Chemical shift imaging (CSI)

Multi-voxel hybrid 2D (CSI) used a PRESS technique for volume localization. The PRESS-selected region was chosen to include as much of the contrast enhanced lesion as possible, as well as contralateral and other normal tissues, while avoiding bone, subcutaneous fat, or other materials that would complicate shimming and water suppression.

2.2. Histopathological examination

All 30 patients were subjected to surgical intervention; 22 of them were subjected to complete resection of the lesions, and 8 of them were biopsied. Histopathological results were performed and correlated with imaging findings.

2.3. Statistical analysis

The collected data were computerized and statistically analyzed using SPSS program (Statistical Package for Social Science) version 18.0. Qualitative data were represented as frequencies and relative percentages. Chi square test was used to calculate difference between qualitative variables. Quantitative data were expressed as mean ± SD (Standard deviation). ANOVA *F*-test test was used to calculate difference between quantitative variables in more than two groups in normally distributed data.

Kappa test (*k*-test) was used to calculate agreement between two different diagnostic tools. *P* value of >0.05 indicates non-significant results.

3. Results

Our study included 30 patients, (18 males, 60%, and 12 females, 40%). Their age ranged between 6 and 76 years (mean of age was 38.16 ± 18.34 year-old), and age groups were distributed as following: 9 patients (30%) below 20 years, 14 patients (46.7%) between 20 and 40 years and 7 patients (23.3%) above 40 years old.

In cases of anaplastic gliomas (13/30) and glioblastoma multiforme (9/30), the lesions appeared with an ill-defined margin, heterogeneous signal intensity with foci of necrosis and hemorrhagic components, surrounded by much edema nearly of grade III and IV and exhibit heterogeneous enhancement pattern on post Gd DTPA series, (Table 1).

When comparing the cMRI results with the histopathological diagnosis in glioma grading, cMRI diagnosed 8 cases of low grade astrocytoma (Fig. 1A–C), with false positive results given in 1 case (proved to be anaplastic astrocytoma), while 13 cases were diagnosed as anaplastic astrocytoma (Fig. 2A), with false positive results given in 3 cases (2 cases proved to be GBM (Fig. 3A and B) and 1 case proved to be low grade glioma. cMRI diagnosed 9 cases with GBM, while histopathological analysis detected 11 cases with GBM, with good agreement between cMRI and histopathological data as Kappa test was 0.80 and statistical significance as *p* value was <0.001 (Table 2).

3.1. Diffusion weighted MR imaging

DWIs using b value 1000 can differentiate different components of the tumor. The necrotic or cystic regions

Table 1
cMRI findings in our cases with their final suggested diagnosis.

Variable	Low grade glioma ($n = 9$)		Anaplastic astrocytoma ($n = 12$)		GBM ($n = 9$)		χ^2	*P*
	N	%	*N*	%	*N*	%		
SI								
Homogenous solid	7	77.7	4	33.3	0	0		
Heterogeneous	0	0	6	50	9	100	17.53	0.002**
Cystic	2	22.2	2	16.6	0	0		
Hemorrhage								
No	9	100	10	83.3	4	44.4	8.12	0.02*
Yes	0	0	2	16.6	5	55.6		
Necrosis								
No	9	100	3	25	0	0	18.46	<0.001**
Yes	0	0	9	75	9	100		
Peri-tumoral edema								
No	5	55.5	0	0	0	0		
Minimal	2	22.2	0	0	0	0	60	<0.001**
Grade I	2	22.2	0	0	0	0		
Grade II	0	0	12	100	0	0		
Grade III–IV	0	0	0	0	9	100		
Mass effect								
Negative	5	55.5	0	0	0	0		
Minimal	2	22.2	0	0	0	0	54.95	<0.001**
Mild	1	22.2	4	33.3	0	0		
Moderate	0	0	8	66.6	0	0		
Marked	0	0	0	0	9	100		
Contrast enhancement								
Negative	1	11.1	0	0	0	0		
Faint	3	33.3	0	0	0	0	60	<0.001**
Mild uniform	5	55.5	0	0	0	0		
Moderate to intense in-homogenous	0	0	12	100	0	0		
Intense in-homogenous	0	0	0	0	9	100		

* Significant ($P < 0.05$).
** Significant ($P < 0.01$).

display DWI hypointensity and had ADCs values ranged from 1.7 to 3.8×10^{-3} mm^2/sec. Enhanced solid regions showed variable hyperintensity on DWIs, and hypointensity on ADC map and had ADCs values in the range of $0.9–1.4 \times 10^{-3}$ mm^2/sec subsequent to variable diffusion restriction according to tumor cellularity.

Regions of peri-tumoral vasogenic edema showed low to high signal intensity on DWIs, and high signal intensity on ADC maps. The ADC values ranged from 1.3 to 2.2×10^{-3} mm^2/sec with lower ADC values in high grade astrocytomas subsequent to peri-tumoral infiltration as seen in anaplastic glioma and GBM.

On the other hand, non-enhancing tumor regions showed high signal intensity on DWIs and variable signal intensity on ADC maps. The ADC values ranged from 1.1 to 1.8×10^{-3} mm^2/sec (Table 3).

Calculated ADC values were accurate in grading of gliomas. ADC values calculated from primary tumoral areas were lowest in GBM (Fig. 3C and D) followed by anaplastic astrocytoma (Fig. 2B and C) and then the low grade type. Low grade gliomas had significantly higher ADC values ($1.5–1.8 \times 10^{-3}$ mm^2/sec.). Cystic gliomas (Fig. 1D and E) ($n = 2$) appeared hyperintense on DWIs (b0), and hypointense on DWIs (b1000) compared to normal appearing brain parenchyma, denoting free diffusion. The ADC values ranged from 2.4 to 3.1×10^{-3} mm^2/sec in the 2 cases denoting no restriction of diffusion. One of the low grade astrocytomas had low ADC value ($1.04–1.2 \times 10^{-3}$ mm^2/sec) denoting restricted diffusion which was correlated with histopathological analysis to be anaplastic glioma.

Restriction of diffusion in peri-tumoral region with minimum ADC value was observed in 10 cases of GBM and only in 7 of the anaplastic glioma grade types with false negative findings in 4 cases and one case respectively (Table 4).

Diffusion MRI with ADC value was found to be more accurate than cMRI in glioma grading, correlated with histopathological diagnosis as it provided a mean ADC value for each tumor grade (Table 4).

3.2. MR spectroscopy

In all gliomas, the relative signal intensity of Cho peak showed a statistically significant increase from low grade

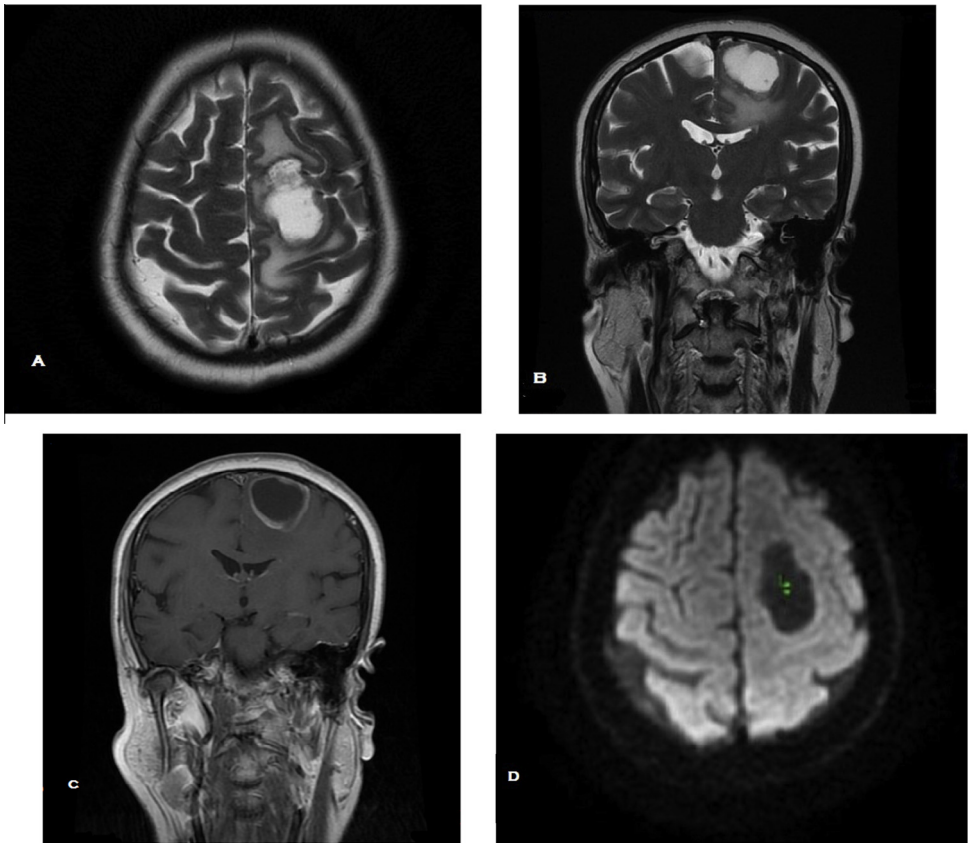

Fig. 1. Cystic glioma (WHO Grade I) in a 9-year-old female patient presented by headache; (A and B) Axial and coronal T2WIs show well demarcated intra-axial cystic lesion of high signal intensity at the left parietal region, surrounded by (grade I) perilesional edema. (C) Coronal T1WI post Gd DTPA revealed marginal enhancement of the cystic lesion. (D and E) Axial DWI (b1000) and ADC map: reveal low signal intensity and hyperintense signal respectively of the cystic lesion in keeping with normal facilitated diffusion while there is subtle restriction of diffusion in the wall of the cyst as is high signal intensity on DWI and low signal intensity on ADC map. Measured ADC value was 2.4 (ROI 1) in the cyst while it was 1.5 in the enhanced wall (ROI 2). (F) SVS (270 ms): there is mild reduction in NAA and Cr peaks associated with elevation of Cho peak. A lactate doublet (Lac) was observed at 1.33 ppm. No peritumoral infiltration was detected.

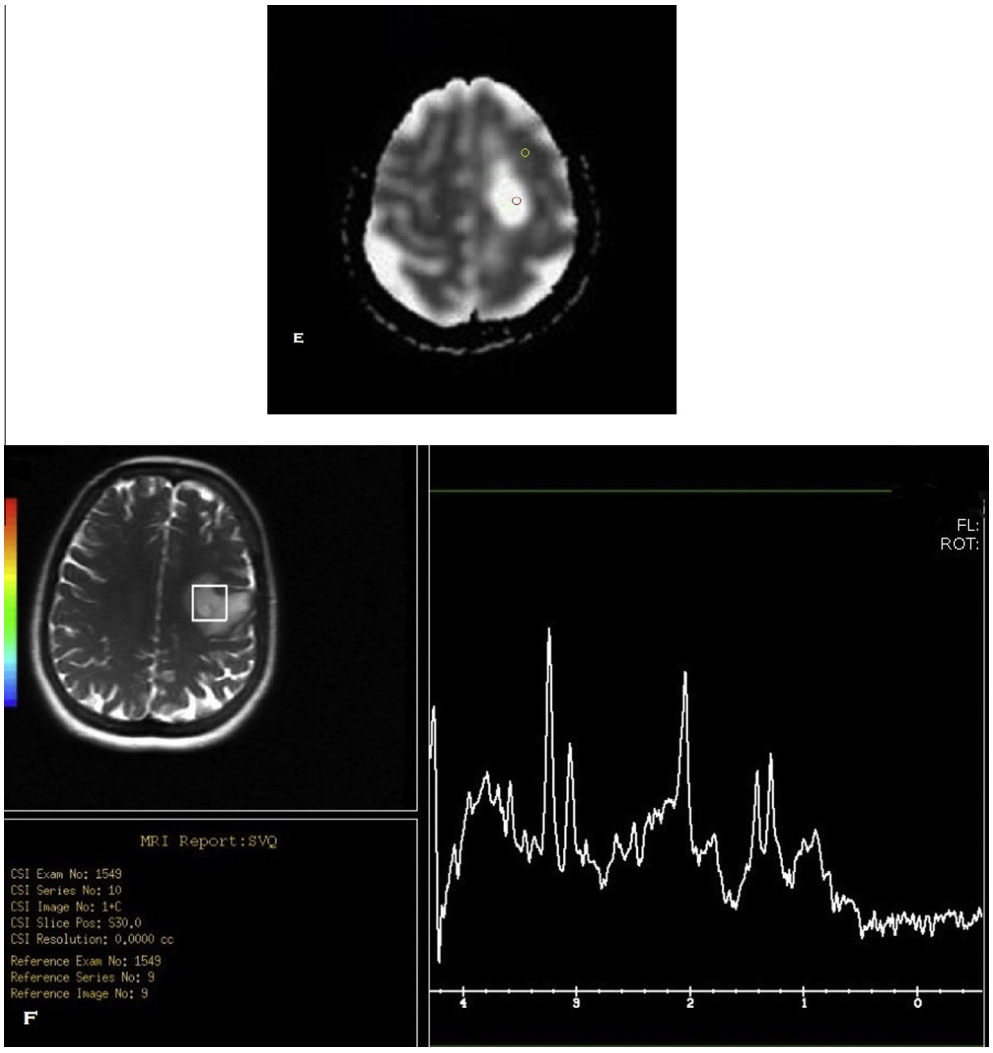

Fig. 1 (*continued*)

type to high grade type as well as a decrease in NAA and Cr peaks with statistically significant difference between low and high grade astrocytoma.

MRS diagnosed 9 cases as low grade type, 12 cases as anaplastic astrocytoma and 9 cases as GBM compared to histopathological data. The calculated Cho/NAA and Cho/Cr ratios showed statistically significant increase from low grade glioma (Fig. 1F) to high grade astrocytoma with no statistically significant difference between anaplastic astrocytoma (Fig. 2D) and GBM (high grade types) (Fig. 3E and F) (Table 5).

Lipid signals were detected in 17 patients (6 patients with anaplastic astrocytoma and all patients with glioblastoma multiforme). Low-grade gliomas had no lipid resonance. Lactate signals were detected in all cases of high-grade gliomas, and in only one low-grade glioma.

The metabolite ratios of Cho/Cr and Cho/NAA in the peritumoral edema were statistically significantly different between low grade gliomas (LGGs) and both anaplastic and GBM (HGGs) where high metabolite ratios were detected in 12 cases of anaplastic glioma and 10 cases of GBM correlated with histopathology and are considered to be more accurate and sensitive in assessing peritumoral infiltration than ADC value which revealed false negative results in 4 cases in anaplastic astrocytoma and 1 case of GBM, while MRS has one false positive case; however, there was no statistical significance difference between anaplastic glioma and GBM (Table 5).

The sensitivity, specificity, positive predictive value, negative predictive value of each imaging modality in assessing their validity in glioma grading are shown in Table 6. ADC value revealed 100% sensitivity, specificity, positive predictive value and negative predictive value in correlation with histopathological data.

4. Discussion

In our study, cMRI diagnosed low grade astrocytoma in 8 cases; 2 of them were cystic, anaplastic astrocytoma in

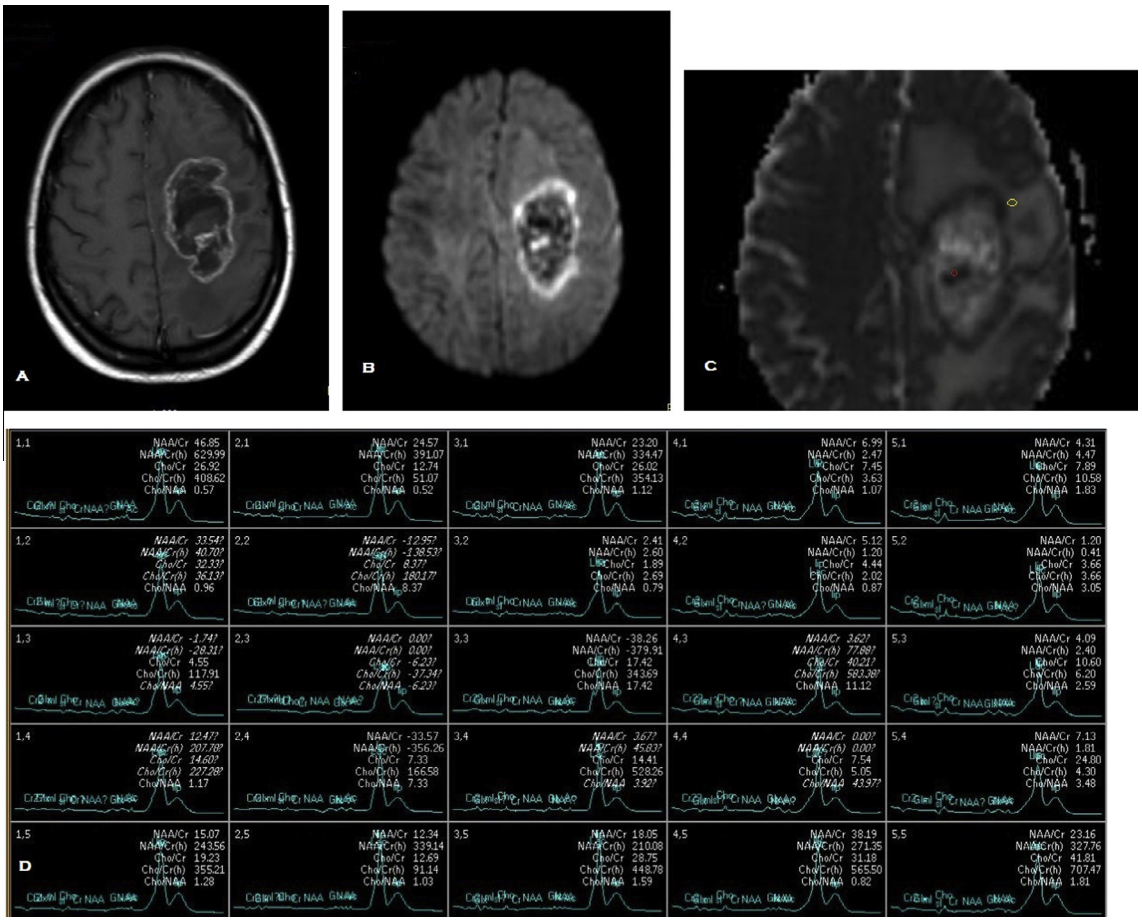

Fig. 2. Left parietal high grade glioma (anaplastic astrocytoma-WHO grade III) in a 45-year-old female patient presented by right-sided weakness; (A) Axial post-contrast T1WIs: show left parietal intra-axial SOL with heterogenous pattern of enhancement and irregular marginal contrast enhancement. (B and C) Axial DWI (b1000) and ADC map: reveal restricted diffusion pattern in the form of heterogenous hyperintense signal on DWI and hypointense signal on ADC map, seen intra-lesional and in the margin of the lesion with cystic changes that display normal facilitated diffusion. ADC value measured in the diffusion restricted area centrally was 1.1. ADC value in the peritumoral edema was non-significant for peritumoral extension (0.7). (D) CSI (270 ms): there is obvious reduction in NAA and Cr peaks associated with elevation of Cho peak. Lipid peak (Lip) at 0.9 was detected in multi-voxels denoting higher grade of malignancy. Also a lactate doublet (Lac) was observed at 1.33 ppm within the cystic part of the lesion. Peritumoral infiltration was detected as the Cho and lips peaks were detected in the peritumoral edema with significant reduction of NAA and Cr.

13 cases and 9 cases as GBM. This grading was based on MR criteria as the signal intensity, peri-tumoral edema, mass effect and the pattern of enhancement.

Histopathological grading is considered the current reference standard of grading which can carry inherent limitations when biopsy samples are not taken from the most malignant part of the tumor or when the tumor is not completely resected. This is a particular problem with glioma because of the infiltrative proliferation of the tumor in high grades. Although histopathological grading is performed on the enhancing portion of the tumor, vascular networks in the peritumoral region serve as a path for tumoral infiltration along perivascular spaces. The region of highest vascularity and malignancy may be then within the so-called peri-tumoral or peri-enhancing region, Wong et al. [3].

When comparing the cMRI results with the histopathological findings regarding the grading of glioma, cMRI diagnosed 8 cases of low grade astrocytoma with false positive results given in 1 case (proved to be anaplastic astrocytoma), while 13 cases were diagnosed as anaplastic astrocytoma with false positive results given in 3 cases (2 cases proved to be GBM and 1 case proved to be low grade glioma). cMRI diagnosed 9 cases with GBM, while histopathological analysis detected 11 cases with GBM. Kappa test of agreement is 0.80 and p value is <0.001, in keeping with good agreement and statistical significance respectively.

Diffusion-weighted imaging was used in our study for evaluation and grading of gliomas by measuring the ADC value in tumoral and peri-tumoral region. The lowest ADC values were seen in glioblastoma multiforme ($n = 11$) and were about $0.75–0.99 \times 10^{-3}$ mm^2/sec (denoting higher cellularity), whereas in anaplastic astrocytoma ($n = 11$) the ADC values were higher ($1.04–1.28 \times 10^{-3}$ mm^2/sec), denoting less cellularity while in low grade glioma the ADC value was in the range of 1.5–1.8 in six cases and 2 cystic glioma types which show no

restriction of diffusion ($2.4–3 \times 10^{-3}$ mm^2/sec) in agreement with Kono et al. [7].

By correlating the diffusion MR imaging findings with histopathological findings, we found similar results in grading of the glioma which were accurate than the preoperative grading by cMRI as false positive diagnosis of one low grade glioma case was detected and false negative diagnosis was detected in one case of anaplastic type and in 2 cases of GBM. The sensitivity, specificity, PPV and NPV were 100% for each.

In the peri-tumoral regions, the inverse correlation between the ADC value and the tumor cellularity was significant in 10 cases of GBM and in 7 cases of anaplastic tumor type with false negative findings in one and 4 cases respectively in agreement with Doskaliyev et al. [15].

MRS provides information about metabolic and histologic markers about the brain or neoplastic ratios. Lip-Lac/Cr values in tumoral area were significantly higher in the high grade astrocytoma group than in pilocytic astrocytoma. There was a trend toward higher Lip-Lac/Lip-lac in tumoral/normal tissue in high grade astrocytoma compared with PA group ($p = 0.06$). There was no statistical significant difference between PA and HGA groups in the remaining metabolite ratios, Aragao et al. [16].

In our study, all tumors showed a decrease in NAA, an increase in Cho and a decrease in Cr peaks. Lactate and

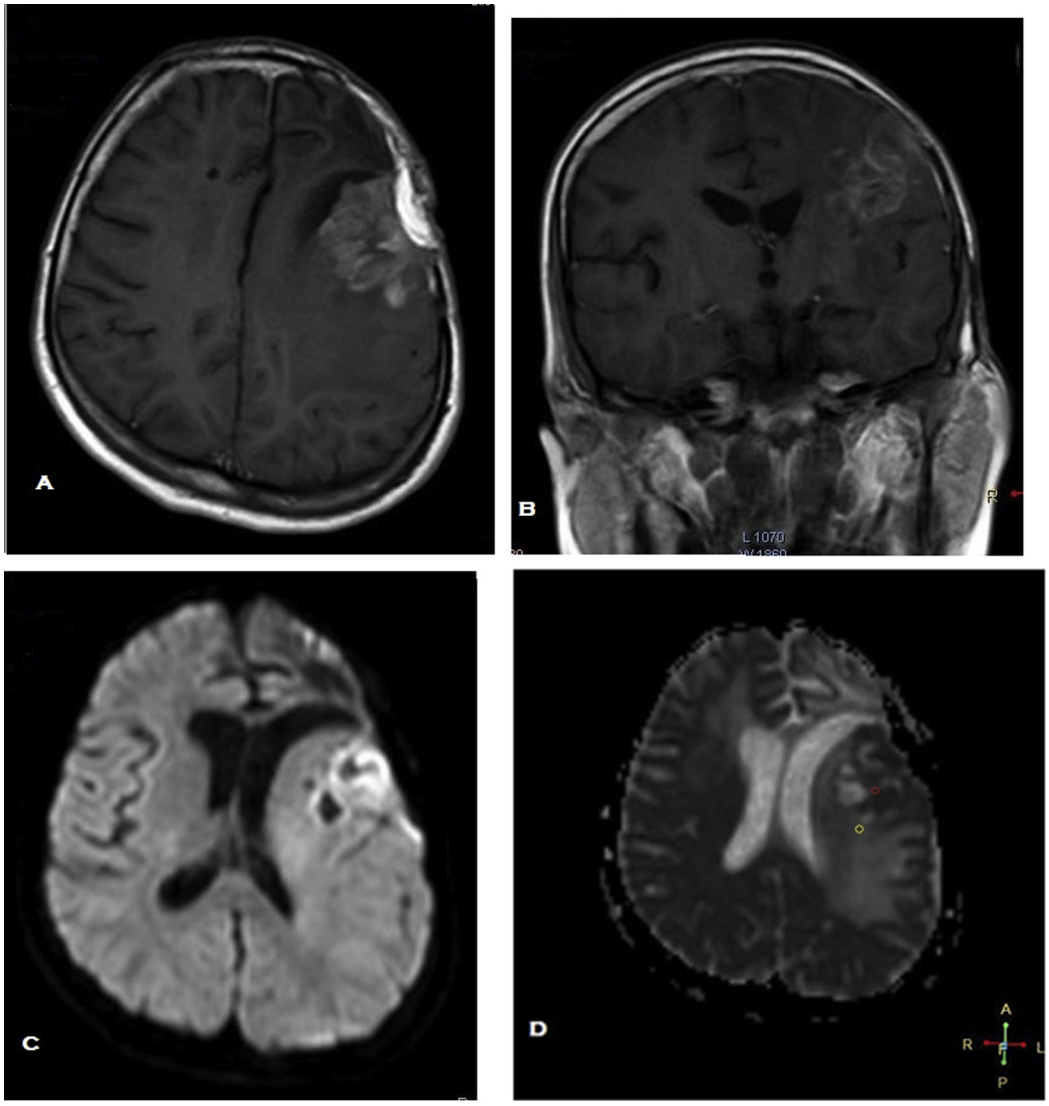

Fig. 3. Left parietal high grade glioma, GBM, (WHO grade IV) in a 55-year-old male patient presented by severe headache and right hemiplegia; (A and B) Axial and coronal post-contrast T1WIs: show ill-defined left parietal SOL with heterogenous enhancement of the solid part. (C and D) Axial DWI (b1000) and ADC map: reveal restricted diffusion pattern in the form of heterogenous hyperintense signal on DWI and hypointense signal on ADC map within the corresponding enhanced solid part. ADC value was 0.9. (E) SVS on the solid enhanced lesion (TE: 270 ms): reveal obvious reduction in NAA and Cr peaks and markedly elevated Cho peak. Significantly elevated lipid peak was detected (Lip) at 0.9, in consistent with higher grade of malignancy. (F) Multi-voxel MRS reveals significant elevated Cho and lipid peaks in the corresponding enhanced solid lesion. Lactate doublets are seen in the cystic part. Peri-lesional infiltration was confirmed by elevated Cho and lipid peaks in the peritumoral edema with reduction on NAA.

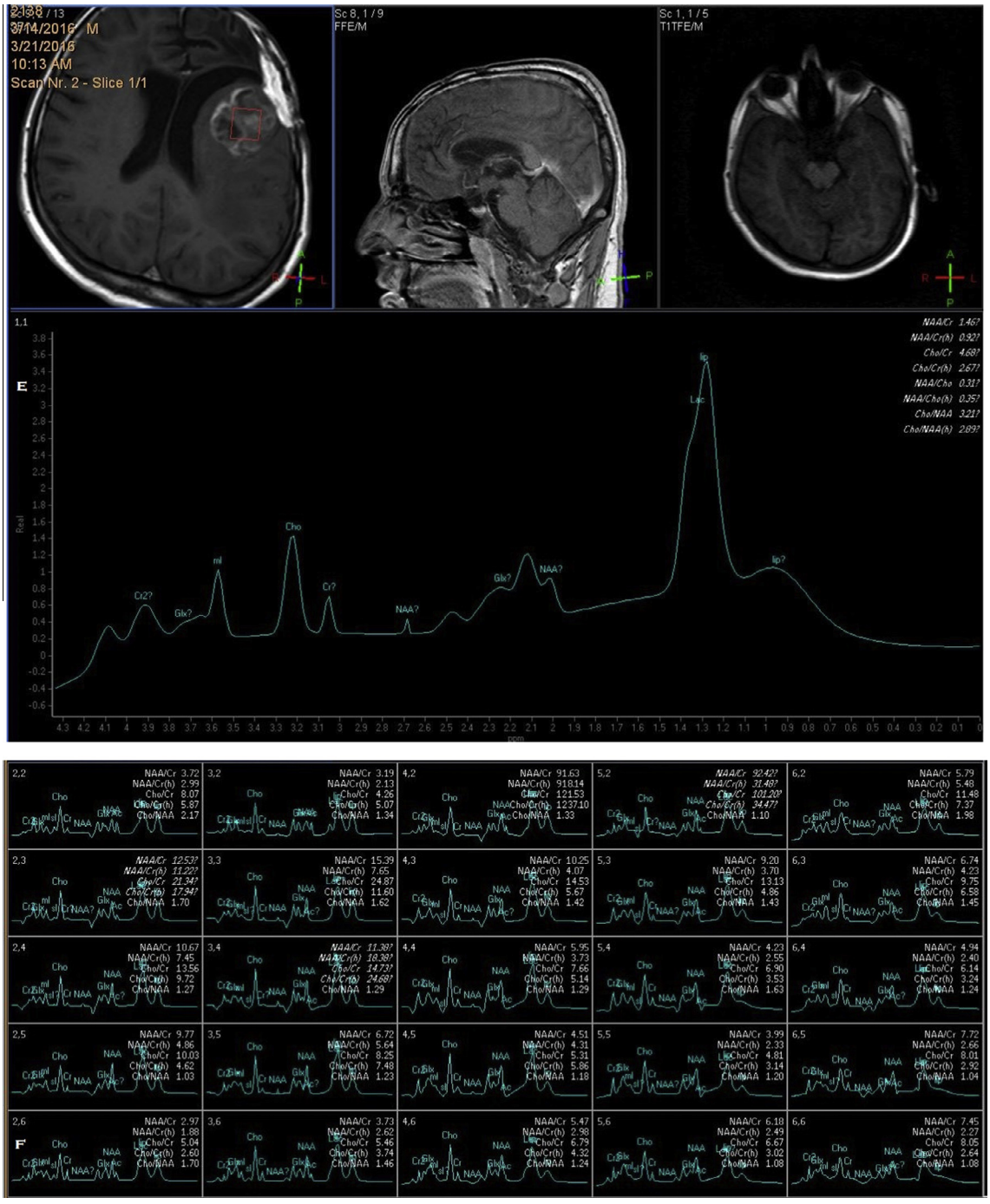

Fig. 3 (*continued*)

lipid peaks are elevated in high grade gliomas as lipid signals were detected in 17 cases of high grade gliomas, 6 cases of anaplastic astrocytoma and in all patients with GBM. None of the low grade gliomas had lipid peak. Lactate signals were detected in all cases of high grade gliomas, and in only one case of low grade glioma.

We detected elevated Cho/NAA and Cho/Cr ratios in tumoral and peritumoral regions of high grade gliomas (anaplastic glioma and GBM) relative to those seen in low grade type with metabolite ratios overlap between anaplastic glioma and GBM. Elevated Lip and lactate peaks were statistical significant in diagnosing high grade glioma than in Low grade gliomas, consistent with Kugel et al. [17] and Kaminogo et al. [18], suggested that Cho/NAA was significantly higher in tumors than in healthy tissues, but could not differentiate the grade of malignancy in gliomas.

Table 2
Comparison of cMRI results with histopathological results regarding the grading of glioma.

Grading of tumor	No. of cases diagnosed by cMRI	No. of cases diagnosed histo-pathologically	Kappa	*P*
Low grade glioma	9	8	0.80	<0.001**
Anaplastic astrocytoma	12	11		
GBM	9	11		
Total	30	30		

** Significant ($P < 0.01$).

Table 3
The appearance of different components of gliomas on DWIs.

Component	SI on DWIs (b0)	SI on DWIs (b1000)	Range of ADC (10^{-3} mm^2/sec.)
Enhancing	High	High	0.90–1.4
Non-enhancing	Intermediate	High	1.1–1.8
Necrotic	High	Low	1.7–3.8
Peri-tumoral edema	High	Low/high	1.3–2.2

N.B the mean ADC value for the normal gray matter, white matter, and CSF is 0.6, 0.8 and 3.0 $\times$ 10^{-3} mm^2/sec. respectively.

Table 4
Comparison of ADC value results with histopathological results regarding the grading of glioma.

Glioma grade type	No. of examined patients by c MRI	ADC value $\times 10^3$ mm^2/sec.	Low ADC in peri-tumoral region	Histo.	Kappa	*P*
Low grade	9	1.5–1.8 (7) 2.4–3 (2)	–	8	0.80	<0.001**
Anaplastic	12	1.04–1.28 (11)	7	11		
GBM	9	0.75–0.99 (11)	10	11		

** Significant ($P < 0.01$).

Table 5
The mean Cho/NAA and Cho/Cr ratios in examined 30 patients with different grades of gliomas.

Glioma grade type	No. of examined patients by MRS	Mean Cho/NAA		Mean Cho/Cr		Histo.	Kappa	*P*
		Tumor	Peri-tumoral edema	Tumor	Peri-tumoral edema			
Low grade	9	4.22 ± 2.85	1.02 ± 0.42	2.55 ± 1.93	1.15 ± 0.42	8	0.85	<0.001**
Anaplastic	12	7.12 ± 3.8	1.8 ± 0.55	3.8 ± 2.6	1.5 ± 0.66	11		
GBM	9	8.12 ± 4.84	2.02 ± 0.65	4.15 ± 2.92	1.92 ± 0.78	11		
F		3.51	8.42	3.53	3.26			
P		0.04*	0.001**	0.04*	0.046*			

* Significant ($P < 0.05$).
** Significant ($P < 0.01$).

Table 6
Validity of cMRI, DWI and ADC and MRS in Grading of Glioma in comparison with histopathology as gold standard test.

Grading	Histo.	Method (Total +ve)	True +ve	False +ve	True −ve	False −ve	Sens. %	Spec. %	PPV %	NPP %	Accuracy
Low grade glioma	8	cMRI (9)	8	1	21	0	87.5	95.5	87.5	95.5	96.7
		DWI&ADC (8)	8	0	22	0	100	100	100	100	100
		MRS (9)	8	1	21	0	100	95.5	88.9	100	96.7
Anaplastic Astrocytoma	11	cMRI (12)	10	3	16	1	90.9	84.2	76.9	94.1	86.7
		DWI&ADC (11)	11	0	19	0	100	100	100	100	100
		MRS (12)	10	2	17	1	90.9	89.5	83.3	94.4	90
GBM	11	cMRI (9)	8	1	18	3	72.7	94.7	88.9	85.7	86.7
		DWI&ADC (11)	11	0	19	0	100	100	100	100	100
		MRS (9)	9	0	19	2	81.8	100	100	90.5	93.3

In our study, Lactate signals were detected in all cases of high-grade gliomas, and in only one case of low grade astrocytoma. This was in agreement with several studies which identified lactate peaks more frequently in high grade gliomas, Gill et al. [19], Frahm et al. [20] and Tien et al. [21], and the amount of lactate was greater with higher grades. However, the significance of the lactate resonance for grading has remained controversial since Kaminogo et al. [18], found lactate in both high and low grade gliomas.

When MRS results were compared with histopathological analysis, we found over- and under estimation in glioma grading as MRS detected 9 cases of low grade glioma while histopathology found only 8 cases with low grade glioma. The false positive findings in one case reflected the presence of mild reduction in NAA and mild elevation of Cho relative to high grade types and lack of lipid or lactate peaks.

Anaplastic astrocytoma detected by MRS in 12 cases showed elevated Lip and lactate peaks like those observed in GBM in spite of the absence of necrosis in some cases and both tumor grades exhibited the very low NAA peak compared to the low grade type. False positive diagnosis was detected in one case which was proved by histopathology as GBM. False negative diagnosis of two cases of GBM by MRS as there was mild lipid and lactate peak, no significant edema by cMRI and NAA mildly decreased and so there was diagnostic confusion as they were graded by histopathology as GBM.

Calculated Cho/Cr ratios showed statistically significant increase from low grade astrocytoma to high grade astrocytoma with no statistically significant difference between high grade astrocytoma types (anaplastic astrocytoma and GBM). The metabolite ratios of Cho/Cr and Cho/NAA in the peritumoral edema were statistically significantly different between low grade gliomas and high grade gliomas and was found to be more accurate than ADC value in detecting peritumoral infiltration in high grade tumors, consistent with Aragao et al. [16].

5. Conclusion

Diffusion MR imaging had higher sensitivity, specificity and accuracy than cMRI and MRS in glioma grading while MRS is more accurate than ADC value in assessing peritumoral infiltration based on high metabolite ratios in the peri-tumoral tissue for anaplastic glioma and GBM, but there was no statistical significance difference between the high grade groups.

Conflict of interest

The authors declared that there is no conflict of interest.

References

[1] Knopp EA, Cha S, Johnson G, Mazumdar A, Golfinos JG, Zagzag D, et al. Glial neoplasms: dynamic contrast-enhanced T2*-weighted MR imaging. Radiology 1999;211:791–8.
[2] Law M, Yang S, Wang H, Babb JS, Johnson G, Cha S, et al. Glioma grading: sensitivity, specificity, and predictive values of perfusion MR imaging and proton MR spectroscopic imaging compared with conventional MR imaging. AJNR Am J Neuroradiol 2003;24 (10):1989–98.
[3] Wong ET, Jackson EF, Hess KR, Schomer DF, Hazle JD, Kyritsis AP, et al. Correlation between dynamic MRI and outcome in patients with malignant gliomas. Neurology 1998;50:777–81.
[4] Dean BL, Drayer BP, Bird CR, Flom RA, Hodak JA, Coons SW, et al. Gliomas: classification with MR imaging. Radiology 1990;147:411–5.
[5] Bulakbasi N, Kocaoglu M, Ors F, Tayfun C, Ucoz T. Combination of single voxel proton MR spectroscopy and apparent diffusion coefficient calculation in evaluation of common brain tumors. AJNR Am J Neuroradiol 2003;24:225–33.
[6] Al-Okaili RN, Krejza J, Wang S, Woo JH, Melhem ER. Advanced MR imaging techniques in the diagnosis of intra-axial brain tumors in adults. RadioGraphics 2006;26:S173–89.
[7] Kono K, Inoue Y, Nakayama K, Shakudo M, Morino M, Ohata K, et al. The role of diffusion-weighted imaging in patients with brain tumors. AJNR 2001;22:1081–8.
[8] Dowling C, Bollen AW, Noworolski SM, McDermott MW, Barbaro NM, Day MR, et al. Preoperative proton MR spectroscopic imaging of brain tumors: correlation with histopathologic analysis of resection specimens. AJNR J Neuroradiol 2001;22:604–12.
[9] Ott D, Henning J, Ernest T. Human brain tumors: assessment with in vivo proton MR spectroscopy. Radiology 1993;186:745–52.
[10] Butzen J, Prost R, Chetty V, Donahue K, Neppl R, Li S-J, et al. Discrimination between neoplastic and nonneoplastic brain lesions by use of proton MR spectroscopy: the limits of accuracy with a logistic regression model. AJNR Am J Neuroradiol 2000;21 (7):1213–9.
[11] Howe FA, Barton SJ, Cudlip SA, Stubbs M, Saunders DE, Murphy M, et al. Metabolic profiles of human brain tumors using quantitative in vivo H-1 magnetic resonance spectroscopy. Magn Reson Med 2003;49(2):223–32.
[12] Galanaud D, Chinot O, Nicoli F, Confort-Gouny S, Fur YL, Barrie-Attarian M, et al. Use of proton magnetic resonance spectroscopy of the brain to differentiate gliomatosis cerebri from low-grade glioma. J Neurosurg 2003;98(2):269–76.
[13] Go KG, Kamman RL, Mooyaart EL, Heesters MA, Pruim J, Vaalburg W, et al. Localized proton spectroscopy and spectroscopic imaging in cerebral gliomas with comparison to PET. Neuroradiology 1995;37:198–200.
[14] Poptani H, Gupta RK, Roy R, Pandey R, Jain VK, Chhabra DK. Characterization of intra-cranial mass lesions with in vivo proton MR spectroscopy. AJNR 1995;16:1593–603.
[15] Doskaliyev A, Yamasaki F, Ohtaki M, Kajiwara Y, Takeshima Y, Watanabe Y, et al. Lymphomas and glioblastomas: differences in the apparent diffusion coefficient evaluated with high b-value diffusion-weighted magnetic resonance imaging at 3T. Eur J Radiol 2012;81 (2):339–44.
[16] Aragao MdeFV, Law M, de Almeida DB, Fatterpekar G, Delman B, Bader ASo RV, et al. Comparison of perfusion, diffusion and MR spectroscopy between low-grade enhancing pilocytic astrocytomas and high-grade astrocytomas. AJNR Am J Neuroradiol 2014;35:1495–502.
[17] Kugel H, Heindel W, Ernestus RI, Bunke J, du Mesnil R, Friedman G. Human brain tumors: special patterns detected with localized ^{1}H MR spectroscopy. Radiology 1992;183:701–9.
[18] Kaminogo M, Ishimaru H, Morikawa M, Ochi M, Ushijiima R, Tani M, et al. Diagnostic potential of short echo time MR spectroscopy of gliomas with single voxel and point-resolved spatially localized proton spectroscopy of brain. Neuroradiology 2000;43:353–63.
[19] Gill SS, Thomas DG, van Bruggen N, Gadian DG, Peden CJ, Bell JD, et al. Proton MR Spectroscopy of intracranial tumors: in vivo and in vitro studies. J Comput Assist Tomogr 1990;14:497–504.
[20] Frahm J, Bruhn H, Hanicke W, Merboldt K, Klaus-Dietmar M, Kay M, et al. Localized proton NMR spectroscopy of brain tumors using short-echo time STEAM sequences. J Comput Assist Tomogr 1991;15:915–22.
[21] Tien RD, Lai PH, Smith JS, Lazeyras F. Single-voxel proton brain spectroscopy exam (PROBE/SE) in patients with primary brain tumors. AJR 1996;167:201–9.